

Shear Stress Correlations in Hard and Soft Sphere Fluids

James. W. Dufty

Department of Physics, University of Florida, Gainesville, FL 32611

(November 13, 2018)

The shear stress autocorrelation function has been studied recently by molecular dynamics simulation using the q^{-n} potential for very large n . The results are analyzed and interpreted here by comparing them to the shear stress response function for hard spheres. It is shown that the hard sphere response function has a singular contribution and that this is reproduced accurately by the simulations for large n . A simple model for the stress autocorrelation function at finite n is proposed, based on the required hard sphere limiting form.

I. INTRODUCTION

The qualitative features of simple atomic fluids are often modelled using the hard sphere pair potential: zero for $q > \sigma$ and infinite for $q < \sigma$. It is well-known that the thermodynamic and structural features of the hard sphere fluid are represented continuously by the soft sphere q^{-n} potential in the limit $n \rightarrow \infty$. In contrast, the dynamical properties for hard and soft sphere fluids are different since the collision time (time required for finite momentum transfer) is strictly zero in the former case and of order $1/n$ in the latter case. As shown below, this has a significant effect on the short time behavior of time correlation functions. Recently, Powles and co-workers [1–3] have investigated the time correlation functions determining the shear and bulk viscosity for the q^{-n} fluid at large values of n (up to $n = 288$). The initial values of these functions diverges $\propto n$, and the simulation results for the normalized correlation functions appear to scale with the single characteristic time $\tau_n \propto 1/n$. These results are puzzling when considered as an approach to the hard sphere

limit. The initial values, i.e. the equal time stress tensor fluctuations, are related to elastic constants which should be finite for the hard sphere fluid. Also, the only time scale in the problem τ_n vanishes for large n leaving no finite time dynamics for the hard spheres fluid. In this picture, the finite Green-Kubo shear viscosity results from the product of the diverging initial condition and a vanishing correlation time. Clearly, the relationship of properties at large n to those at $n = \infty$ must be more complex. The objective here is to resolve these paradoxes by calculating the corresponding properties for the hard sphere fluid directly to allow comparison with those at large n . Attention is restricted to the response function for shear viscosity, but similar results apply for the bulk viscosity response function as well.

Standard methods of linear response lead to Green-Kubo expressions for the shear viscosity as the time integral of a shear response function. For soft spheres this response function is proportional to the autocorrelation function for the microscopic stress tensor. The form of the stress tensor is identified from the microscopic local conservation law for the momentum density. Since it explicitly involves the interparticle force, a divergence for large n can be anticipated. Application of the same linear response methods for the hard sphere fluid lead to several differences:

- The response function is not simply the stress tensor autocorrelation function, as for soft spheres, but has an additional singular contribution proportional to $\delta(t)$.
- The coefficient of the singular contribution can be calculated exactly and is simply related to the limiting form of the stress fluctuations for the soft sphere fluid.
- The form of the microscopic stress tensor for hard spheres is quite different from that for soft spheres, and the initial value of the stress tensor autocorrelation function is finite.
- The hard sphere stress tensor autocorrelation function has a characteristic time scale of the mean free time, which is the same as that for the soft sphere fluid at large n .

The singular part of the hard sphere correlation function evolves continuously from the soft sphere correlation function as $n \rightarrow \infty$, and is closely related to the divergent initial value. The results of Powles et al. are shown to be an accurate measurement of this singular part. However, the resolution of this component in the simulation tends to mask the finite remainder that persists on the mean free path time scale, whose existence is clear from the hard sphere calculations and which is essential for the correct density dependence of transport properties. An alternative representation of the simulation results is proposed to more closely demonstrate the approach to the hard sphere limit.

The relevant features of the dynamics and statistical mechanics of hard spheres are introduced in the next section to provide the necessary definitions and to contrast with the corresponding features for soft spheres. In Section III the results for linear response to a transverse velocity field perturbation are quoted, and the Green-Kubo expression is identified. The singular contribution is evaluated exactly and given a representation appropriate for comparison with the MD simulation results. The remainder, determined from the stress tensor autocorrelation function for hard spheres is evaluated in an Enskog approximation. The limiting form for soft spheres approaching the hard sphere limit is discussed on the basis of these results. Some final comments are offered in Section IV.

It is a pleasure to dedicate this brief contribution to Keith Gubbins - friend, mentor, and colleague - who has played such an important role in unfolding the mysteries of transport in simple and complex fluids.

II. STATISTICAL MECHANICS OF HARD SPHERES

Any interatomic potential with discontinuities (e.g., hard sphere, square well) implies an infinite force at the point of discontinuity. Consequently, the usual formulation of Newtonian dynamics in terms of forces alone is no longer appropriate. In this section the dynamics and statistical mechanics for a system of N smooth hard spheres with diameter σ is reviewed briefly [4].

The dynamics consists of free streaming until a given pair i, j is in contact, at which point the relative velocity of that pair changes instantaneously according to the elastic collision rule

$$\tilde{\mathbf{g}}_{ij} = \mathbf{g}_{ij} - 2\hat{\boldsymbol{\sigma}}(\mathbf{g}_{ij} \cdot \hat{\boldsymbol{\sigma}}) \quad (1)$$

Here $\mathbf{g}_{ij} = \mathbf{v}_i - \mathbf{v}_j$ is the relative velocity for particles i and j . The state of the system at time t is completely characterized by the positions and velocities of all spheres at that time and is represented by a point in the associated $6N$ dimensional phase space, $\Gamma_t \equiv \{\mathbf{q}_1(t), \dots, \mathbf{q}_N(t), \mathbf{v}_1(t), \dots, \mathbf{v}_N(t)\}$. The sequence of free streaming and binary collisions determines uniquely these positions and velocities of the spheres at time t for given initial conditions. A more complete notation expressing this dependence on initial conditions is $\Gamma_t(\Gamma_0)$. Observables of interest are represented by the phase functions $A(\Gamma_t(\Gamma))$, and their average for given statistical initial data at $t = 0$ is defined by

$$\langle A(t); 0 \rangle \equiv \int d\Gamma \rho(\Gamma) A(\Gamma_t(\Gamma)), \quad (2)$$

where $\rho(\Gamma)$ is the probability density or ensemble for the initial state, normalized to unity. An equivalent representation of this average is obtained by changing variables to integrate over Γ_t rather than over Γ expressed as a function of Γ_t , i.e. $\Gamma = \Gamma_t^{-1}(\Gamma_t)$. This change of variables in (2) allows the time dependence to be expressed in terms of the probability density

$$\langle A(t); 0 \rangle \equiv \int d\Gamma \rho(\Gamma, t) A(\Gamma) = \langle A; t \rangle, \quad (3)$$

where the probability density at time t is defined by $\rho(\Gamma, t) \equiv \rho(\Gamma_t^{-1}(\Gamma))$. The Jacobian of the transformation is unity. All of the above is the same for both hard and soft spheres.

The equilibrium time correlation functions for observables A and B are defined by

$$C_{AB}(t) \equiv \langle \delta A(t) \delta B \rangle_e = \int d\Gamma \rho_e(\Gamma) \delta A(t) \delta B, \quad \delta X \equiv X - \langle X \rangle_e. \quad (4)$$

where $A(t) = A(\Gamma_t(\Gamma_0))$. The Gibbs distribution given by

$$\rho_e(\Gamma) = W(\{q_{ij}\}) \prod_i \phi(v_i), \quad \phi(v_i) = \left(\frac{\beta m}{2\pi}\right)^{3/2} e^{-\beta m v_i^2/2} \quad (5)$$

is a stationary state for the hard sphere dynamics. The "overlap" function $W(\{q_{ij}\})$ is defined to vanish if any pair overlap, $q_{ij} < \sigma$, and is normalized to unity when integrated over all configuration space. The equilibrium correlation function is stationary

$$\langle \delta A(t) \delta B \rangle_e = \langle \delta A \delta B(-t) \rangle_e \quad (6)$$

where $B(-t) = B(\Gamma_{-t}(\Gamma))$ has the time reversed dynamics.

For practical purposes it is useful to identify the generators L_{\pm} and \bar{L} for the two representations, defined for $t > 0$ by

$$A(\pm t) \equiv e^{\pm L_{\pm} t} A(\Gamma), \quad \rho(\Gamma, t) = e^{-\bar{L} t} \rho(\Gamma). \quad (7)$$

These are not the usual generators of Hamilton's equations for continuous forces and are somewhat more complex due to the singular nature of hard spheres. They are given by

$$L_{\pm} = \sum_{i=1}^N \mathbf{v}_i \cdot \nabla_i \pm \frac{1}{2} \sum_{i=1}^N \sum_{j \neq i}^N T_{\pm}(i, j), \quad \bar{L} = \sum_{i=1}^N \mathbf{v}_i \cdot \nabla_i - \frac{1}{2} \sum_{i=1}^N \sum_{j \neq i}^N \bar{T}(i, j). \quad (8)$$

The first terms on the right sides generate free streaming while the second terms describe velocity changes. The three binary collision operators, $T_{\pm}(i, j)$ and $\bar{T}(i, j)$, for particles i and j are given by

$$T_{\pm}(i, j) = \mp \sigma^2 \int d\Omega \Theta(\mp \mathbf{g}_{ij} \cdot \hat{\boldsymbol{\sigma}})(\mathbf{g}_{ij} \cdot \hat{\boldsymbol{\sigma}}) \delta(\mathbf{q}_{ij} - \boldsymbol{\sigma})(b_{ij} - 1), \quad (9)$$

$$\bar{T}(i, j) = \sigma^2 \int d\Omega \Theta(\mathbf{g}_{ij} \cdot \hat{\boldsymbol{\sigma}})(\mathbf{g}_{ij} \cdot \hat{\boldsymbol{\sigma}}) [\delta(\mathbf{q}_{ij} - \boldsymbol{\sigma}) b_{ij} - \delta(\mathbf{q}_{ij} + \boldsymbol{\sigma})], \quad (10)$$

where $d\Omega$ denotes the solid angle integration for the unit vector $\hat{\boldsymbol{\sigma}}$, \mathbf{r} is the relative position vector of the two particles, and the operator b_{ij} is a substitution operator, $b_{ij} F(\mathbf{g}_{ij}) = F(b_{ij} \mathbf{g}_{ij})$, which changes the relative velocity $\mathbf{g}_{ij} = \mathbf{v}_i - \mathbf{v}_j$ into its scattered velocity according to (3) $b_{ij} \mathbf{g}_{ij} = \widetilde{\mathbf{g}}_{ij}$. For continuous potentials all generators are the same $L_{\pm} = \bar{L}$ but for hard spheres all three generators clearly are different.

The local microscopic conservation laws follow from the above dynamics by differentiating the local conserved densities of mass, energy, and momentum with respect to time. The relevant conservation law for the discussion here is that for momentum density

$$\partial_t p_\alpha(\mathbf{r}, \pm t) + \partial_j \tau_{\pm\alpha\beta}(\mathbf{r}, \pm t) = 0, \quad (11)$$

$$\mathbf{p}(\mathbf{r}) = \sum_{i=1}^N \mathbf{p}_i \delta(\mathbf{r} - \mathbf{q}_i), \quad \partial_j \tau_{\pm\alpha\beta}(\mathbf{r}) = \mp L_{\pm} p_\alpha(\mathbf{r}) \quad (12)$$

The subscript \pm distinguishes the forms of the momentum flux for the case $t > 0$ and $t < 0$. The detailed expression for $\tau_{\pm ij}(\mathbf{r}, t)$ is not required below, only its volume integral

$$\begin{aligned} \mathcal{T}_{\pm\alpha\beta} &\equiv \int d\mathbf{r} \tau_{\pm\alpha\beta}(\mathbf{r}) \\ &= \sum_{i=1}^N m v_{i,\alpha} v_{i,\beta} + \frac{1}{2} \sigma^3 \sum_{i \neq j}^N \int d\Omega \Theta(\mp \mathbf{g}_{ij} \cdot \hat{\sigma}) m (\mathbf{g}_{ij} \cdot \hat{\sigma})^2 \hat{\sigma}_\alpha \hat{\sigma}_\beta \delta(\mathbf{q}_{ij} - \sigma) \end{aligned} \quad (13)$$

This form for the hard sphere momentum flux(es) can be contrasted with that for the soft sphere potential $v(q) = \epsilon (\sigma/q)^n$

$$\mathcal{T}_{\alpha\beta} = \sum_{i=1}^N m v_{i,\alpha} v_{i,\beta} + \frac{1}{2} \sum_{i \neq j}^N \hat{q}_{ij\alpha} \hat{q}_{ij\beta} n \epsilon \left(\frac{\sigma}{q_{ij}} \right)^n \quad (14)$$

which can be written for large n as

$$\mathcal{T}_{\alpha\beta} = \sum_{i=1}^N m v_{i,\alpha} v_{i,\beta} + n \frac{1}{2} \sigma \epsilon \sum_{i \neq j}^N \int d\Omega \hat{\sigma}_\alpha \hat{\sigma}_\beta \delta(\mathbf{q}_{ij} - \sigma) \quad (15)$$

While (13) and (15) are similar, both involving a surface integral for pairs of particles at contact, there are two significant differences. The hard sphere stress tensor is momentum dependent and the soft sphere stress tensor is proportional to n , diverging in the large n limit.

III. LINEAR RESPONSE

The results of the last section now allow a discussion of the response functions for the hard sphere fluid. Attention here is restricted to the response to an initial transverse perturbation

of the velocity field, $u_y(x, 0) = A \sin(x/\lambda)$. The velocity field for λ much larger than the mean free path and for times long compared to the mean free time then obeys the diffusion equation

$$\partial_t u_y(x, t) + (\eta/n_e m) \nabla^2 u_y(x, t) = 0 \quad (16)$$

where η is the shear viscosity and n_e is the equilibrium density. The derivation of this result is straightforward using the standard methods of linear response and the Liouville dynamics defined in the last section. The details will be given elsewhere [5] and only the results discussed here. The shear viscosity is given by the Green-Kubo expression

$$\eta = \beta \left[-\frac{1}{V} \langle \mathcal{T}_{+xy} \Lambda_{xy} \rangle_e + \int_0^\infty dt \frac{1}{V} \langle \mathcal{T}_{+xy}(t) \mathcal{T}_{-xy} \rangle_e \right] \quad (17)$$

where

$$\Lambda_{xy} = \int d\mathbf{r} x p_y(\mathbf{r}) = \sum_{i=1} q_{ix} m v_{iy} \quad (18)$$

For soft spheres $\mathcal{T}_{+xy} = \mathcal{T}_{-xy} = \mathcal{T}_{xy}$ and $\langle \mathcal{T}_{xy} \Lambda_{xy} \rangle_e = 0$ since \mathcal{T}_{xy} is independent of the particle velocities while Λ_{xy} is an odd function of the velocities. Thus, the usual Green-Kubo form for the shear viscosity in terms of the time integral of the stress tensor autocorrelation function is regained

$$\eta^{ss} = \beta \int_0^\infty dt \frac{1}{V} \langle \mathcal{T}_{xy}(t) \mathcal{T}_{xy} \rangle_e \quad (19)$$

In contrast, $\langle \mathcal{T}_{+xy} \Lambda_{xy} \rangle_e$ does not vanish for hard spheres. The equivalence of (17) and (19) in the limit of $n \rightarrow \infty$ requires

$$\lim_{n \rightarrow \infty} \frac{1}{V} \langle \mathcal{T}_{xy}(t) \mathcal{T}_{xy} \rangle_e = -\frac{2}{V} \langle \mathcal{T}_{+xy} \Lambda_{xy} \rangle_e \delta(t) + \frac{1}{V} \langle \mathcal{T}_{+xy}(t) \mathcal{T}_{-xy} \rangle_e \quad (20)$$

This is the primary observation of this work regarding the relationship of shear response for soft and hard spheres. The hard and soft sphere stress autocorrelation functions differ by a singular term.

To explore this relationship, two results are noted. First, for hard spheres the coefficient of the singular term can be calculated exactly to get [5]

$$-\frac{2}{V} \langle \mathcal{T}_{+xy} \Lambda_{xy} \rangle_e = \frac{4}{5} \sigma \left(\frac{m}{\beta \pi} \right)^{1/2} (p - p^k). \quad (21)$$

Also, for soft spheres the exact initial condition is [6]

$$\frac{1}{V} \langle \mathcal{T}_{xy}(0) \mathcal{T}_{xy} \rangle_e \equiv \frac{1}{\beta} G_\infty = \frac{1}{\beta} \left[p^k + \frac{1}{5} (n-3) (p - p^k) \right]. \quad (22)$$

Here $\beta = 1/k_B T$, $p^k = n_e/\beta$, p is the pressure

$$p = p^k \left(1 + \frac{2}{3} \pi n_e^* \chi \right), \quad (23)$$

and χ is the equilibrium pair correlation function evaluated at $q_{ij} = \sigma$. Equation (22) shows the divergence of the high frequency shear modulus, G_∞ , as $n \rightarrow \infty$. Furthermore, the dominant short time behavior of $\langle \mathcal{T}_{xy}(t) \mathcal{T}_{xy} \rangle_e$ for soft spheres with large n is

$$\langle \mathcal{T}_{xy}(t) \mathcal{T}_{xy} \rangle_e = \langle \mathcal{T}_{xy}(0) \mathcal{T}_{xy} \rangle_e \left[1 - \left(\frac{t}{\tau_n} \right)^2 + \text{order } t^4 \right] \quad (24)$$

with the characteristic short time scale

$$\tau_n = \frac{\sigma \sqrt{\beta m}}{n} = \frac{\tau_1}{n} \quad (25)$$

Comparison of (21) and (22) shows the relationship

$$\lim_{n \rightarrow \infty} \frac{4\tau_n}{\sqrt{\pi}} \frac{1}{V} \langle \mathcal{T}_{xy}(0) \mathcal{T}_{xy} \rangle_e = \left(-\frac{2}{V} \langle \mathcal{T}_{+xy} \Lambda_{xy} \rangle_e \right) \quad (26)$$

Note that the left side is finite in this limit due to the factor of $\tau_n \approx 1/n$.

These results provide an appropriate means to discuss and interpret the simulation results of reference [3]. The stress tensor autocorrelation function is written as

$$\langle \mathcal{T}_{xy}(t) \mathcal{T}_{xy} \rangle_e = \langle \mathcal{T}_{xy}(0) \mathcal{T}_{xy} \rangle_e C_n(t) \quad (27)$$

and the simulation data is reported for the normalized correlation function $C_n(t)$ (a subscript n has been included since the simulations are performed for $n = 18, 36, 72, 144$, and 288). It is found that the results are globally well-fit by

$$[C_n(t)]_{sim} \approx \text{sech} \left(a \frac{t}{\tau_n} \right). \quad (28)$$

where $a = \pi^{3/2}/4 \approx 1.4$ (in reference [3] $a = \sqrt{2}$). This is the puzzling result mentioned in the Introduction above. The coefficient of $C_n(t)$ in (27) diverges for large n while $[C(t)]_{sim}$ is a "universal" function of time with a vanishing time scale. To understand this paradoxical behavior combine (26) - (28) to get, for large n

$$\begin{aligned} \left[\frac{1}{V} \langle \mathcal{T}_{xy}(t) \mathcal{T}_{xy} \rangle_e \right]_{sim} &= \left(-\frac{2}{V} \langle \mathcal{T}_{+xy} \Lambda_{xy} \rangle_e \right) \frac{\sqrt{\pi}}{4\tau_n} \operatorname{sech} \left(a \frac{t}{\tau_n} \right) \\ &= \left(-\frac{2}{V} \langle \mathcal{T}_{+xy} \Lambda_{xy} \rangle_e \right) \delta_n(t) \end{aligned} \quad (29)$$

In the second line $\delta_n(t)$ is a representation of the delta function as $n \rightarrow \infty$ defined by

$$\delta_n(t) = \frac{a}{\pi\tau_n} \operatorname{sech} \left(a \frac{t}{\tau_n} \right) \quad (30)$$

It is now clear that the MD simulation has measured the singular contribution on the right side of (20). This reinterpretation of the MD results shows a remarkable confirmation of the hard sphere singular contribution evolving continuously from the soft sphere stress autocorrelation function. It also demonstrates the role of the diverging shear modulus in constructing the amplitude of $\delta_n(t)$. Finally, the paradox of the vanishing time scale is now understood as well. The second term on the right side of (20) is expected to have a time scale of the order of the mean free time (see below), but has not been well-resolved by the simulations. The normalization to define $C(t)$, appropriate to identify this singular term, makes observation of the second term difficult since it then vanishes as n^{-1} . Still, such deviations from the fit (28) are observed in the simulations, as noted below.

The second term in (20) is the hard sphere stress autocorrelation function. It can be evaluated approximately from Enskog kinetic theory. The details will be given elsewhere, and only the result quoted here

$$\frac{1}{V} \langle \mathcal{T}_{+xy}(t) \mathcal{T}_{-xy} \rangle_e \rightarrow \beta^{-1} p^k \left(1 + \frac{2}{5} \frac{p - p^k}{p_k} \right)^2 e^{-t/\tau_{mfp}} \quad (31)$$

where τ_{mfp} is the mean free time

$$\tau_{mfp} = \frac{5}{24} \frac{p_k}{(p - p^k)} \sqrt{\pi} \tau_1. \quad (32)$$

The pressures for the hard and soft sphere fluids are continuously related for large n so both the non-singular part in (31) and the mean free path should be similar in both cases. It is easily verified that use of (31) and (21) in the Green-Kubo expression (17) yields the exact Enskog shear viscosity. Both the singular term and the stress auto correlation function contribute at intermediate velocities. In the low density limit the singular contribution to the viscosity vanishes and only the stress autocorrelation function contributes. Also, note that the value at $t = 0$ for the hard sphere stress autocorrelation function is finite, in contrast to that for the soft sphere correlation function. The implications of this for elastic constants will be discussed elsewhere.

The hard sphere results suggest how to write an approximate stress autocorrelation function for the soft sphere potential at large n . There should be two contributions with two different time scales. The first is that which has been determined from the simulations and which yields the singular contribution in the hard sphere limit. It also gives entirely the exact short time behavior. The second term should vanish at short times, but tend toward the form (31) for $t \gg \tau_n$. A simple approximation consistent with the above exact properties and which has the proper hard sphere limit is

$$\frac{1}{V} \langle \mathcal{T}_{xy}(t) \mathcal{T}_{xy} \rangle_e \approx \frac{1}{\beta} G_\infty \operatorname{sech} \left(a \frac{t}{\tau_n} \right) + X \left(\frac{t}{\tau_n} \right) \frac{p^k}{\beta} \left(1 + \frac{2p - p^k}{5 p_k} \right)^2 e^{-t/\tau_{mfp}}. \quad (33)$$

Equivalently, the normalized correlation function is

$$C_n(t) \approx \operatorname{sech} \left(a \frac{t}{\tau_n} \right) + \Delta_n(t) \quad (34)$$

where $\Delta_n(t)$ is the contribution from the non-singular part

$$\Delta_n(t) = X \left(\frac{t}{\tau_n} \right) \frac{p^k}{G_\infty} \left(1 + \frac{2p - p^k}{5 p_k} \right)^2 e^{-t/\tau_{mfp}} \quad (35)$$

The function $X(t)$ controls the crossover from the time scale τ_n to the mean free time scale. For consistency it must be even in time, vanish up through order t^2 , and approach unity for large times. One simple form with these properties is

$$X(t) = \left(\frac{t^2}{1 + t^2} \right)^2 \quad (36)$$

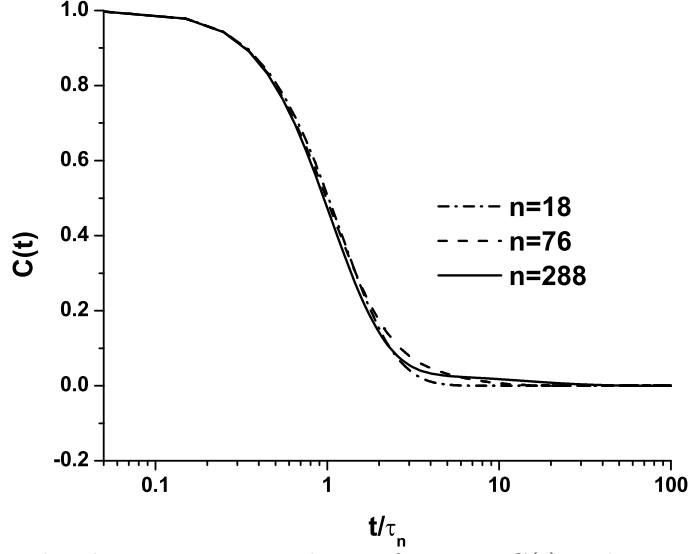


FIG. 1. Plot of normalized stress autocorrelation function $C(t)$ vs $\log t$ at packing fraction 0.45 for $n = 18, 76,$ and 288

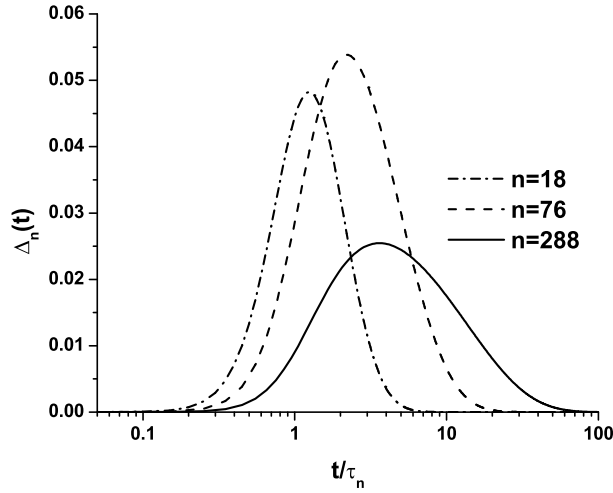


FIG. 2. Same as Fig1 for $\Delta(t)$, non-singular contribution to $C(t)$

For illustration, Figure 1 shows $C_n(t)$ as a function of t/τ_n for $n = 18, 76,$ and 288 at the packing fraction $\pi n_e \sigma^3/6 = 0.45$. This is quite similar to the simulation results in Figure 5 of reference [3]. The small variations with n for $t/\tau_n > 1$ are due to $\Delta_n(t)$. The latter is shown in Figure 2.

A more rational choice for the crossover function $X(t)$ is obtained by relating it to the low density autocorrelation function

$$X\left(\frac{t}{\tau_n}\right) = e^{t/\tau_{mfp}^{(0)}} \left[C^{(0)}(t) - \operatorname{sech}\left(a\frac{t}{\tau_n^{(0)}}\right) \right] \quad (37)$$

The superscript (0) denotes the low density limit. For example, $\tau_n^{(0)}$ is the time scale obtained from the expansion of the low density autocorrelation function to second order in t . With this choice the normalized stress autocorrelation function becomes

$$C_n(t) \approx \operatorname{sech}\left(a\frac{t}{\tau_n}\right) + \left[C^{(0)}(t) - \operatorname{sech}\left(a\frac{t}{\tau_n^{(0)}}\right) \right] \frac{p^k}{G_\infty} \left(1 + \frac{2p - p^k}{5p^k}\right)^2 e^{-t/\tau}. \quad (38)$$

where the new time scale of the second term is

$$\frac{1}{\tau} = \frac{1}{\tau_{mfp}} - \frac{1}{\tau_{mfp}^{(0)}} = \frac{24}{5\sqrt{\pi}\tau_1} \left(\frac{p - p^k}{p^k}\right) \quad (39)$$

The calculation of $C^{(0)}(t)$ for all times is still a difficult problem, but one that has been reduced to two particle dynamics. The remaining terms are all expressed in terms of the pressure. It should be interesting to see how well (38) predicts the density dependence of the viscosity for the soft sphere fluid.

IV. DISCUSSION

On purely physical grounds it is clear that the physical properties of the soft sphere fluid for large n should approach those of the hard sphere fluid, in general. This requires that the continuous Newtonian dynamics of the soft sphere fluid must generate the singularities that are inherent in the dynamics of the hard sphere fluid. The molecular dynamics simulation results of references [1–3] provide the first direct demonstration of how such singular properties can be extracted from competition between diverging fluctuations (the high frequency shear modulus) and a vanishing collision time. More generally, the autocorrelation functions for the soft sphere fluid have contributions on two time scales, τ_n and τ_{mfp} . For asymptotically short times only the former contributes. There is then a crossover to longer

times when the latter dominates. As the density increases, τ_{mfp} decreases and if n is not large the two times can become comparable and the dynamics is a composition of both. This is the case in Figure 2 for $1 \lesssim t/\tau_n \lesssim 10$. A reevaluation of the simulation data to extract the non-singular dynamics on the time scale τ_{mfp} is of some interest and could be compared directly to hard sphere simulations at $t > 0$. It appears that a recently proposed approximation [7] to interpolate correlation functions between their exact short time dynamics and long time exponential decay does not work in this case due to the divergent initial value.

Similar questions regarding the relationship of hard and soft sphere systems can be raised for the solid state. The elastic constants are usually related to the stress tensor fluctuations which diverge for the soft sphere fluid but are finite for the hard sphere fluid. To clarify this, the exact relations (20) and (26) can be combined to give

$$\lim_{n \rightarrow \infty} \left[\frac{1}{V} \langle \mathcal{T}_{xy}(t) \mathcal{T}_{xy} \rangle_e - \frac{1}{V} \langle \mathcal{T}_{xy}(0) \mathcal{T}_{xy} \rangle_e \frac{4\tau_n}{\sqrt{\pi}} \delta_n(t) \right] = \frac{1}{V} \langle \mathcal{T}_{+xy}(t) \mathcal{T}_{-xy} \rangle_e \quad (40)$$

The right side is finite for $t = 0^+$ (38), which suggests that the proper elastic properties of the soft sphere fluid require subtraction of the short time dynamics with the diverging amplitude. This can be viewed as an annealing process on the time scale τ_n .

The analysis of simulation data for thermal conductivity and bulk viscosity for the soft sphere fluid leads to similar results. The description will be given in a more detailed report on this topic elsewhere [5].

V. ACKNOWLEDGEMENTS

The author is indebted to J. Powles and D. Heyes for communication of results prior to publication. This research was supported in part by National Science Foundation grant PHY 9722133.

[1] D. Heyes and J. G. Powles, *Molec. Phys.* **95**, 259 (1998).

- [2] J. G. Powles, G. Rickayzen, and D. Heyes, Proc. R. Soc. Lond. A **455**, 3725 (1999).
- [3] J. G. Powles and D. Heyes, Mol. Phys. **98**, 917 (2000).
- [4] M. Ernst, J. Dorfman, W. Hoegy, and J. van Leeuwen, Physica 45, 127 (1969); J. Sengers, M. Ernst, and D. Gillespie, J. Chem. Phys. **56**, 5583 (1972).
- [5] J. Dufty, (to be published).
- [6] R. Zwanzig and R. Mountain, J. Chem. Phys. 43, 4464 (1965).
- [7] R. Nettleton, J. Phys. A: Math. Gen. **33**, 7555 (2000).